

A Reliability-Based and Stochastic Optimization for Balancing Capacity and Uncertainties in a Roof-Mounted Photovoltaic (PV) System

Zilong Zhao¹, Guoquan Lv^{2*}, Yanwen Xu³, Pingfeng Wang⁴

1 Trane Technologies Company LLC, Davidson, NC 28036, USA

2 Department of Architecture, Zhejiang University, Hangzhou 310058, China

3 Department of Mechanical Engineering, University of Texas at Dallas, Richardson, TX, 75080, USA

4 Department of Industrial and Enterprise Systems Engineering, University of Illinois at Urbana-Champaign, Urbana, IL 61801, USA
(Corresponding Author: guoquanlv@intl.zju.edu.cn)

ABSTRACT

Photovoltaic (PV) systems are being increasingly adopted in buildings, but the installed capacity often fails to account for uncertainties during the usage phase. A novel probabilistic optimization model based on the reliability level is applied to size the PV arrays on a residential building. The minimum total installation area of the PV panels is treated as the objective of the optimization. To consider the impacts of various uncertainties during the installation and continuous operations of PV system, a design variable, installation angle, and multiple environmental variables, including annual solar irradiation, ambient temperature, and attenuation rate on the system efficiency, are integrated into the model. A unique statistic profile of uncertainty is established for each of the variables based on the verifications from the documented literature. In the meantime, to concurrently ensure the sufficient electricity supply provided by the PV system and mitigating the system degradation, constraints on the total power generation, self-use power ratio, and temperature increase were formulated. By establishing different levels of confidential reliability and magnitudes of uncertainties associated with design and random variables, the optimized size and installed angle of PV exhibited significantly different results.

Keywords: solar energy, design optimization, reliability, probabilistic model, building energy

NONMENCLATURE

Abbreviations

Pr	Probability
PV	Photovoltaic

Symbols

A	PV installation area, m ²
---	--------------------------------------

B	Building
D	Design variables
f, T	function
i	Time step, hour; or index
j	Variable index
P	Power, kW
R	Reliability
t	Target
U	Variable Space
X	Random variables
μ	Mean value
σ	Standard deviation
β	Installed angle, °
γ	Azimuth angle, °
η	Efficiency

1. INTRODUCTION

As the urgent call for carbon reduction in mitigating building energy consumption gains priority, along with the advancements in photovoltaic (PV) technology, PV is considered a crucial solution to future energy challenges [1-3]. Concurrently, more and more buildings are choosing to install PV systems. This is due to their proximity to places of energy consumption and the suitability of building rooftops for such installations. Therefore, the optimal sizing of solar PV systems is a crucial task, which requires careful consideration of various technical, economic, and environmental factors to ensure their effective integration within the energy landscape. Oversizing the system can lead to excessive investment and underutilization of resources [4,5], while undersized array can result in unsatisfied energy demands. As documented in many existing studies [6,7], fluctuations in annual solar irradiation, errors made during installation, the attenuation of component efficiency, etc. may largely affect the total power

generation of the PV array. However, rare current studies addressed the uncertainties due to time change or construction errors of these variables during the optimization process [8,9], especially when it comes to the integration of building electricity energy profile and random disturbances from ambient environment in addition to weather conditions. In a sophisticated sizing process of PV array, it is necessary to consider the uncertainties behind the design parameters and ambient site parameters that may affect the performance of the PV system.

To achieve the right balance, the assessment of dynamic parameters such as solar irradiance patterns, local climatic conditions, building energy consumption profiles, etc. is necessary. However, the current design of rooftop photovoltaic (PV) system capacity often underrates these crucial factors that can impact the system's performance during operation. This study proposes an integration of reliability-based design optimization (RBDO) method in the design of residential solar system. RBDO is widely adopted in the field of mechanical design [10-13]. Instead of aiming at a deterministic optimization, it considers the real-world uncertainties that may impose risks in the device of interest performing normal functions. The proposed novel optimization model identifies the optimal design configurations of roof-mounted PV while assessing the reliability of the system under the above-mentioned uncertainties from the environment and the design process.

2. RELIABILITY-BASED ANALYSIS

2.1 Optimization algorithms

As mentioned above, by taking into account the uncertainties, the optimization can be achieved with higher fidelity and reliability. Similar to a regular optimization approach, the objective function, the boundary constraints, and the mandatory simulation parameters are required to complete the algorithm. In this study, the goal of the simulation is to reduce the PV investment while maintaining the minimum power supply to the building. Therefore, the minimization of the required installation area of PV panels is regarded as the objective function, which can be calculated by dividing the to-be-fulfilled building electricity energy demand by the produced power from PV, presented by Eqs. (1) and (2).

$$f = \text{minimize } A_{PV}(D, X) \quad (1)$$

$$A_{PV} = \frac{\text{Sum}(P_B)}{\text{Mean}(P_{PV})} \quad (2)$$

where D and X denote the arrays for design variables (ones that can be varied at design phase) and random variables (environmental factors). In the meantime, the total demand on the PV productions is set to be 70% of the building loads in this study. The constraint function, on the other hand, is established based on the ratio of produced power to the power demand over a one-year simulation span. The alignment of the dynamic profile of PV power supply and the building energy profile is recognized as a key to measure whether the residential PV is effective. In this work, the calculated PV power are used to calculate the alignment ratio, which can be expressed by Eq (3).

$$\text{Ratio}_{Total} = \frac{1}{8760} \sum_{i=1}^{8760} P_{PV}(i) / \text{Max}(P_{total}(\beta)) \quad (3)$$

where "i" denotes the hourly data point, ranging from 1 to 8760; P_{total} denotes the totally generated PV power which is a function of installation angle. And when considering the sole factor, the potentially maximum power that can be generated $\text{Max}(P_{total}(\beta))$ is used to measure the percentage of the real generated power at the end of the optimization. To ensure the effectiveness of PV, P_{Ratio} is set to be at least higher than a threshold value. Therefore, the constraint function can then be formulated as:

$$\text{Pr}(P_{Ratio} - \text{threshold} \geq 0) = R^t \quad (4)$$

where Pr represents the probability of the constraint function being satisfied, and R^t represents the target reliability. In this case, R^t is set to vary between primarily 0.80 to 0.85. Thus, when the target reliability is set to be 85%, the optimization is conducted under the prerequisite that the PV can fulfill at least 70% of the building electricity demand at an 85% confidential reliability level. Furthermore, the other constraint is set to be the value of the PV self-generation ratio, which is defined by Eq. (5). It is used to ensure that the PV generated power can be effectively used by the building in real time [14]. There is also a third constraint, which is the increase of PV back panel temperature. As widely recognized, when the temperature increases, the PV efficiency may be significantly affected.

$$\text{Ratio}_{Self-use} = \frac{1}{8760} \sum_{i=1}^{8760} \frac{\text{Min}(P_{PV}(i), P_B(i))}{P_B(i)} \quad (5)$$

By using First Order Reliability Method (FORM), the variables indexed with probability distribution are firstly transformed into the Euclidean space, becoming the standard distribution variables.

$$U_i = T(D_i \& X_i) = \frac{D_i \& X_i - \mu_{D_i \& X_i}}{\sigma_{D_i \& X_i}} \quad (6)$$

The searching gradient of the algorithm can be then computed based on the impacts of design variables on the objective function. The searching point can then be updated in the next iteration.

$$\begin{aligned} \frac{\partial \beta_i}{\partial D_j} &= \frac{\partial (U^T U)^{1/2}}{\partial D_j} \Big|_{U = u * G_j(U)=0} \\ &= \frac{U^T \partial U}{\beta_i \partial D_j} \Big|_{U = u * G_j(U)=0} \end{aligned} \quad (7)$$

2.2 Model configurations

The building simulation is carried out in Trace3DPlus [15] using a high-rise apartment construction. In this specific study, the uncertainties are involved in multiple parameters including inclination angle of the installed PV panels, solar azimuth angle, the intensity fluctuations in the solar irradiation, variations in the ambient temperature, and the actual electricity conversion efficiency of the panels. Note that among these factors, the panels' inclination angle is treated as design variable since it can be adjusted by the designers, while the remaining ones are treated as random variables, which are not under manual control despite their non-negligible impacts on the ultimate performance of the PV system. In a typical RBDO algorithm, a probabilistic index is used to represent the distribution of values for each concerned variable. In this study, normal distribution is used for all design and random variables. The mean values and standard deviations, accompanied with the lower and upper bounds for design variable are shown in Table 1.

Take angle of installation, β , and efficiency coefficient, Coef- η , as two examples, the first guessed value for β is 45° and it is the only design variable that needs to be optimized. The range of its potential value varies from -90° to 90° . The uncertainty in the installation process itself is exhibited as a standard normal distribution with a standard deviation (STD) of 2° . Similarly, Coef- η is also treated as a probabilistic variable that has a mean value of 18% and 1% STD during the optimization process.

Table 1. Parameter configurations in RBDO (baseline).

Design Variable D & Random Variable X	Initial Guess	Mean Values/Lower and Upper Bounds	Standard Deviations
β	45°	$(-90^\circ, 90^\circ)$	2°
γ	335°	335°	2°
Coef-R	1.0	1.0	0.1
Coef-T	1.0	1.0	0.1
Coef- η	0.18	0.18	0.1

2.3 Details on model constraints

To regulate the optimization, unlike deterministic process, RBDO uses the combination of constraint functions, probabilistic variable indices, and the confidential reliability level to achieve an ultimate optimization that can balance the objective and the uncertain risks in the system. As mentioned above, in this study, three constraints were applied to ensure the PV system operates in an economic and sustainable way. The first constraint is defined as that the overall ratio of total PV-generated power over building electrical demand, as expressed in Eq.4, should not be lower than 60%. The second constraint is defined as that the self-use ratio, which is the ratio of effective part of the generated power over the transient building demand at the same time (Eq.5), should not be lower than 50%. The third constraint is that the increase of back panel temperature, which may lead to system deterioration, should be below 19°C . Note that the temperature setting here aims to show an example of how the constraint of panel temperature influence the design optimization. The three constraints aim to regulate optimization and avoid extreme design that leads to either less effective solar absorption or excessively high temperature.

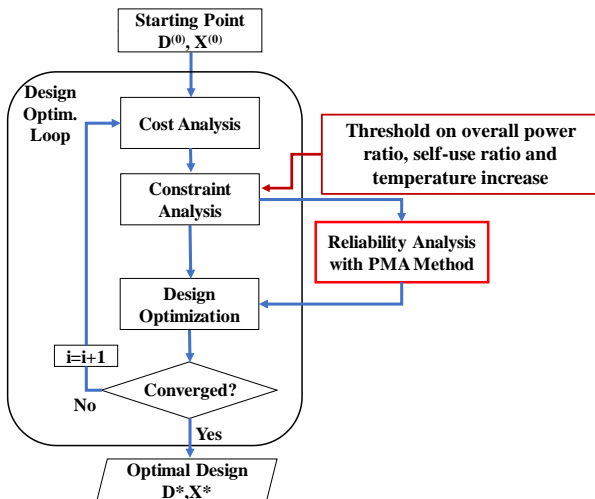


Fig. 2 Simulation flowchart using RBDO on optimizing the PV sizing parameters [10].

3. OPTIMIZATION RESULTS

Fig. 2 presents the residuals for the three constraints—overall power ratio, self-use ratio, and increase of back panel temperature under the 80% reliability and baseline scenario. The variations of these residuals are plotted over the iterations. Note that all constraints’ residuals converge steadily to negative values, which indicates the effectiveness of the optimization. To be more specific, the overall power ratio ultimately reaches 74.1% at the end of optimization, which is higher than the threshold, 60%. The self-use ratio reaches 61.2%, and the increase of panel temperature is controlled exactly at the threshold, 19°C. Note that when conducting a deterministic optimization, the temperature increase may be easily elevated beyond such tolerance and potentially lead to component degradation.

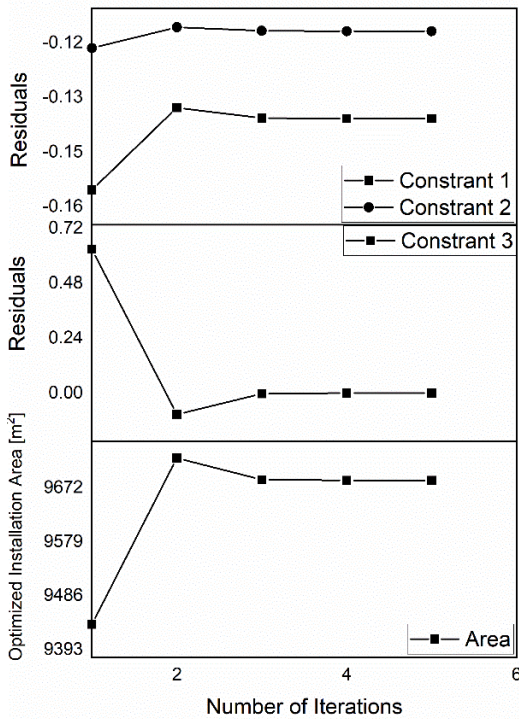


Fig. 2 Residuals of constraints and optimization of installed area of PV over simulation iterations when reliability is set to be 80% in the baseline case.

The objective, installed area of PV panels, also shows a fluctuation during the first few iterations, which indicates that the solver is seeking for a design point that can concurrently and sufficiently satisfy the three constraints, which lead to more conservative design configurations, therefore at the second iteration, the area increases to be 9723.3 m². However, when the optimization is complete, the area is minimized to 9684.7 m². The optimal installed angle, in this scenario, turns out to be 51.35°. It apparently deviates from the deterministically optimized value, which is 22°. However,

when establishing the temperature constraint and system reliability, the algorithm takes into account the uncertainties associated with the random variables and thus alters the optimization results.

Furthermore, to compare how different reliability levels and magnitudes of uncertainties associate with variables’ standard deviations, aside from baseline, an additional case is created using high uncertainties. As mentioned earlier, Tab.1 presents the uncertainty configurations in the baseline case, while in the high uncertainty case, all the STDs are doubled. In the meantime, when considering no uncertainty, the results from deterministic scenario are also presented for comparison. As demonstrated by Tab.2, when coupling 60%, 70%, and 80% reliability with the three scenarios, the optimized results are completely different. As one can observe, when high uncertainty exists in key parameters such as solar irradiation profile and ambient temperature, when optimizing under the 80% reliability, compared to B-60%, the optimal angle is increased from 38.3° to 61.9° to avoid excessive temperature increase. The installed area exhibits a significant increase of 10.6% from 9257.5 m² to 10238 m². If compared to the deterministic case (8964.2 m²), the increase in the installed area reaches up to 14.2%. The overall power ratio at the end of optimization shows a trend of decline when reliability increases.

Table 2. Optimization results that are based on different reliability levels (60% to 80%) for the deterministic case (A), the baseline case (B), and the high-uncertainty (H) case.

Cases	Installation Angle	Installed Area (m ²)	Overall ratio
A	22°	8964.6	0.885
B-60%	38.3°	9257.5	0.832
B-70%	45.5°	9454.3	0.789
B-80%	51.4°	9684.7	0.741
H-60%	45.2°	9441.6	0.792
H-70%	54.4°	9836.9	0.710
H-80%	61.9°	10238	0.629

A comparison is also made between the small variations and large variations in the reliability levels. Fig.3 shows the changes in five parameters—four variables and one objective—under the variation of reliability at different intervals. The results, on the other hand, show similarity to that was observed earlier. When reliability increases, the installed angle is elevated, and the installed area is increased. However, this results in the reduction of overall power ratio and self-use ratio, with the temperature constraints satisfied in all cases.

uncertainties. To be more specific, when applying high uncertainties in the design and random variables, the overall ratio decreases from 88.5% to 62.9%.

- d) By satisfying the temperature constraint, the optimized installed angle of PV panels is lifted from approximately 22° to over 60° under higher uncertainties and reliability.

ACKNOWLEDGEMENT

The authors gratefully acknowledge the funding support from Zhejiang Provincial Key R&D Program (No. 2021C03147). The modeling process is supported by the computing infrastructure of Trane Technologies Company LLC.

REFERENCE

[1] Shen C., Lv G., Zheng K., Ruan C., Zhang C., and Dong Y. 2022. Modeling and investigating the detailed characteristics of solar lighting/heating system based on spectrum split of nanofluids. *EBE*. 3 (1), 30-39. <https://doi.org/10.1016/j.enbenv.2020.10.003>

[2] Zhao Z., Lin Y., Stumpf A., and Wang X. 2023. Improving LEED-certified building loads on borehole heat exchangers by coupling subsurface variables. *Appl. Therm. Eng.* 224, 120119. <https://doi.org/10.1016/j.applthermaleng.2023.120119>

[3] Zhao Z., Stumpf A., Lin Y., and Wang X. 2022. Impacts of prospective LEED building's energy loads on a borehole heat exchanger: A case study in Central Illinois. *Proceedings of the IGSHPA Research Track 2022*. <http://dx.doi.org/10.22488/okstate.22.000030>

[4] López-Castrillón W., Sepúlveda H. H., and Mattar C. 2022. Too many solar panels? Oversizing or undersizing of hybrid renewable energy systems based on different sources of information. *Sustain. Energy Technol. Assessments*. 52, 102264. <https://doi.org/10.1016/j.seta.2022.102264>

[5] Shivaie M., Mokhayeri M., Kiani-Moghaddam M., and Ashouri-Zadeh A. 2019. A reliability-constrained cost-effective model for optimal sizing of an autonomous hybrid solar/wind/diesel/battery energy system by a modified discrete bat search algorithm. *Sol. Energy*. 189 (1), 344-356. <https://doi.org/10.1016/j.solener.2019.07.075>

[6] Al-falahi M. D. A., Jayasinghe S. D. G., and Enshaei H. 2017. A review on recent size optimization methodologies for standalone solar and wind hybrid renewable energy system. *Energy Conv. Manag.* 143 (1), 252-274. <https://doi.org/10.1016/j.enconman.2017.04.019>

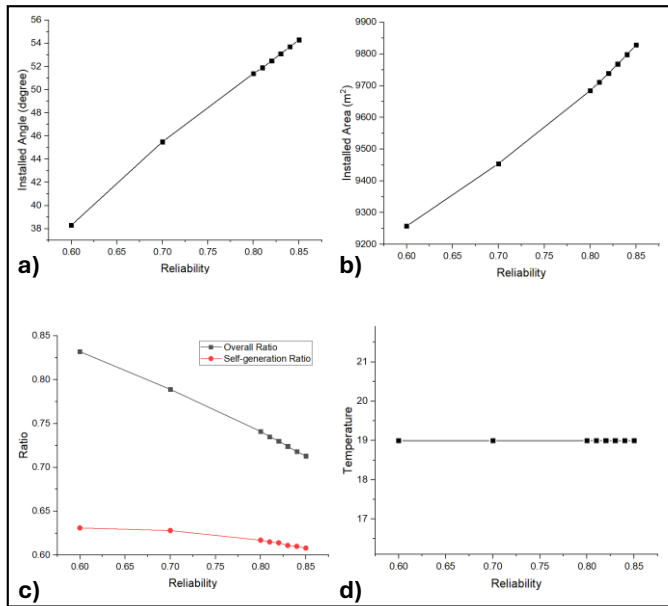


Fig. 3 Parameters in the baseline case with varied reliability levels.

4. CONCLUSIONS

This study proposes a novel optimization method to minimize the required installation area of residential PV panels, while concurrently considering the uncertainties associated with design variable (installed angle) and multiple random variables. Under the effect of constraint functions, the optimized installed angle and installed area show non-negligible differences among different scenarios. The main conclusions can be drawn below.

- a) The feasibility of combining the deterministic PV sizing model with a reliability-based optimization approach is validated with convergence reached in all tested scenarios.
- b) The optimized installed area tends to be increased by up to 14.2% considering the limit in the increase of PV back panel temperature.
- c) The overall power ratio and self-use ratio tend to decrease when carrying out the optimization under higher reliability and higher

- [7] Podder B., Biswas A., and Saha S., Multi-objective optimization of a small sized solar PV-T water collector using controlled elitist NSGA-II coupled with TOPSIS. *Sol. Energy*. 230, 688-702.
<https://doi.org/10.1016/j.solener.2021.10.078>
- [8] Gao G. and Huang H. 2024. Stochastic optimization for energy economics and renewable sources management: A case study of solar energy in digital twin. *Sol. Energy*. 262 (15), 111865.
<https://doi.org/10.1016/j.solener.2023.111865>
- [9] Zhao Z., Lv G., Xu Y., Lin Y., Wang P., Wang, X. 2024. A Stochastic Optimization Model for a Ground Source Heat Pump System with Uncertainty Quantifications on Transient Geologic Variables. Stanford University. SGP-TR-227.
- [10] Zhao Z., Xu Y., Lin Y., Wang X., and Wang P. 2021. Probabilistic modeling and reliability-based design optimization of a ground source heat pump system. *Appl. Therm. Eng.* 197, 117341.
<https://doi.org/10.1016/j.applthermaleng.2021.117341>
- [11] Zhao Z., Lv G., Xu Y., Lin Y., Wang P., Wang, X. 2024. Enhancing ground source heat pump system design optimization: A stochastic model incorporating transient geological factors and decision variables. *Renew. Energy*. 225, 120279.
<https://doi.org/10.1016/j.renene.2024.120279>
- [12] Zhao Z., Lin Y., Stumpf A., and Wang X. 2023. Assessing impacts of groundwater on geothermal heat exchangers: A review of methodology and modeling. *Renew. Energy*. 190, 121147.
<https://doi.org/10.1016/j.renene.2022.03.089>
- [13] Xu Y., Kohtz S., Boakye J., Gardoni P., Wang P. 2023. Physics-informed machine learning for reliability and systems safety applications: State of the art and challenges. *Reliab. Eng. Syst. Saf.* 230, 108900.
<https://doi.org/10.1016/j.ress.2022.108900>
- [14] Lv G., Zhao Z., Zhao K., Ge J. 2024. The Building Decarbonization in High-Density Cities: Challenges and Solutions. *J. Eng. Sustain. Build. Cities*. 5(4): 040801.
<https://doi.org/10.1115/1.4066503>
- [15] TRACE® 3D Plus. Accessed 2024. Retrieved from: <https://www.trane.com/commercial/north-america/us/en/products-systems/design-and-analysis-tools/trane-design-tools/trace-3d-plus.html>